Pharmacogn. Mag.
A multifaceted peer reviewed journal in the field of Pharmacognosy and Natural Products
www.phcog.com | www.phcog.net

ORIGINAL ARTICLE

GC–MS Metabolomics and Network Pharmacology-Based Investigation of Molecular Mechanism of Identified Metabolites from *Tinospora cordifolia* (Willd.) Miers for the Treatment of Kidney Diseases

Gaurav[1,2], Mohammad Umar Khan[2,3], Parakh Basist[1,2], Sultan Zahiruddin[1,2], Mohammad Ibrahim[2], Rabea parveen[4], Anuja Krishnan[5], Sayeed Ahmad[1,2]

[1]Centre of Excellence (CoE) in Unani Medicine (Pharmacognosy and Pharmacology), [2]Bioactive Natural Product Laboratory, School of Pharmaceutical Education and Research, [3]Department of Food and Technology, School of Interdisciplinary Science and Technology, [4]Department of Pharmaceutics, School of Pharmaceutical Education and Research, [5]Institute of Molecular Medicine, School of Interdisciplinary Science and Technology, Jamia Hamdard, New Delhi-110062, India

Submitted: 18-Dec-2021 Revised: 18-Feb-2022 Accepted: 29-Mar-2022 Published: 19-Sep-2022

ABSTRACT

Background: *Tinospora cordifolia* (Willd.) Miers (*T. cordifolia*) is a well-known Indian medicinal plant containing several nonpolar and polar constituents that play an important role to mitigate various ailments, such as diabetes, urinary disorders, and hepatoprotective. Due to the lack of evidence on phytopharmacological relevance to the unpredicted nonpolar matrix of *T. cordifolia*, the present study aimed to evaluate the metabolomic pattern of different fractions obtained from aqueous extract of *T. cordifolia,* which has been recommended in AYUSH for various ailments including kidney disorders. **Materials and Methods:** High-performance thin-layer chromatography and gas chromatography–mass spectrometry (GC–MS) analyses were performed on aqueous extracts and hexane, dichloromethane, and methanolic fraction of *T. cordifolia* aqueous extract to evaluate fingerprinting and metabolomic profile. Principal components and pharmacokinetic analysis were performed using XLSTAT and *in-silico* SwissADME tool to determine metabolite variability and pharmacokinetic relationship based on lipophilicity and drug-likeness. Further, network pharmacology analysis was performed to determine the exact biomolecular relationship of T. cordifolia in alleviating kidney disease. **Results:** The GC–MS metabolomics results showed several metabolites in different fractions with high variability of phytoconstituents in the methanolic fraction. In pharmacokinetics, each metabolite exhibited a direct correlation between drug lipophilicity and permeability. Network pharmacological suggested five fatty acids, which significantly interacted with the genes such as AGTR1, ATG, RELA, NOS3, NOS2, REN, INS, IL6, TNF, MAPK1, and CASP3, which could potentially regulate various pathophysiological conditions, such as hypertension, insulin resistance, oxidative and inflammatory stress, and electrolyte homeostasis, thereby strengthening the normal function of the kidney. **Conclusion:** The study showed that six metabolites of *T. cordifolia* play a multimechanistic role in alleviating kidney disease.

Key words: Fatty acids, GC–MS, metabolomics, network pharmacology, *Tinospora cordifolia* (Willd.) Miers

SUMMARY

- Since history, medicinal plants are contributing an immense role in the alleviation of several acute and chronic ailments due to their multi-mechanistic and therapeutic effect. Among thousands of traditionally reported medicinal plants, *T. cordifolia* is a well-known Indian traditional medicinal plant used for several ailments including kidney diseases. Due to a lack of phytopharmacological and molecular-based evidences of *T cordifolia* in the alleviation of kidney disease, the study aimed to explore metabolomics pattern and their biological significance in kidney disease. The metabolomic study was conducted through GC-MS analysis while network pharmacology analysis was conducted to explore the multi-mechanistic and therapeutic effect of *T. cordifolia* in the alleviation of kidney disease and its associated complications. the results showed that the metabolites such as fatty acids, terpenes, monoterpenes, monoterpenoid aldehyde, phenylpropanoid, anthracene, organics acids, etc were found as major metabolites of *T. cordifolia*. Network pharmacology analysis showed that fatty acids (oleic acid, linoleic acid, lauric acid, methyl palmitate, etc.) and phenylpropanoid (cinnamaldehyde) exhibited a significant effect in the alleviation of kidney disease via regulation of the genes involved in its pathophysiology such as oxidative stress, inflammatory stress, vascular rigidity, apoptosis, positive regulation cell death, etc. Hence, it can be demonstrated that the aforementioned metabolites of *T. cordifolia* can be the best leads for alleviating kidney disease and associated complications.

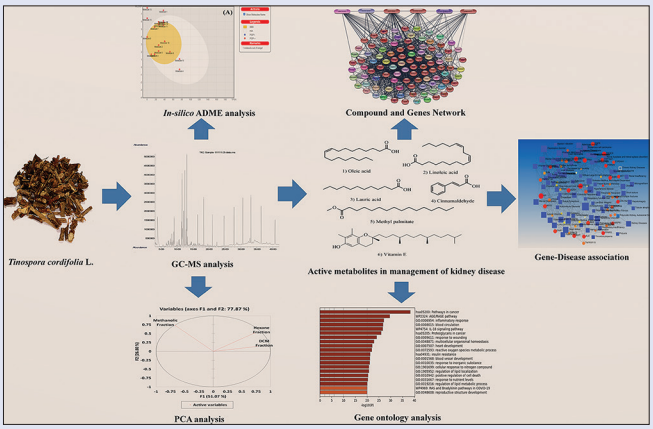

Abbreviations used: MS: mass spectrometry, NMR: nuclear magnetic resonance, HPTLC: high-performance thin-layer chromatography, GC–MS: gas chromatography–mass spectrometry, TM: traditional medicine, PCA: principal component analysis, HCA: hierarchical cluster analysis, TPSA: topological polar surface area, GO: gene ontology, PPI: protein–protein interaction, MCA: multiple correspondence analysis,

Cite this article as: Gaurav, Khan MU, Basist P, Zahiruddin S, Ibrahim M, Parveen R, *et al.* GC–MS metabolomics and network pharmacology-based investigation of molecular mechanism of identified metabolites from *Tinospora cordifolia* (Willd.) Miers for the treatment of kidney diseases. Phcog Mag 2022;18:548-58.

BBB: blood–brain barrier, ESRD: end-stage renal disease, and ECs: endothelial cells.

Correspondence:

Dr. Sayeed Ahmad,
Department of Pharmacognosy and Phytochemistry, School of Pharmaceutical Education and Research, Jamia Hamdard, New Delhi - 110 062, India.
E-mail: sahmad_jh@yahoo.co.in
DOI: 10.4103/pm.pm_582_21

Access this article online
Website: www.phcog.com
Quick Response Code:

INTRODUCTION

Metabolomics is a comprehensive analytical technique for the quality assessment of targeted or untargeted metabolites in a biological system.[1] Metabolomic studies have been concomitant with many research fields, including functional genomics, environmental and biological stress studies, integrative systems, and biology biomarker discovery.[2,3] Besides, such analytical studies are gaining exponential growth in the field of quality control analysis of phytoconstituents diversity present in medicinal plants.[4] Medicinal plants are typically composed of a complex mixture of different varieties of phytoconstituents, such as fatty acids, carotenoids, steroids, terpenoids, alkaloids, phenols, flavonoids, and glycosides. However, it still remains a challenge to validate herbal medicine or products based on their quality, safety, and regulatory aspects.[3-6] Although, the most common analytical techniques such as chromatography, mass spectrometry (MS), and nuclear magnetic resonance (NMR) are used abundantly in quantitative and quantitative estimation of plant metabolites. Having said that, these techniques are the main object of choice which are greatly hyphenated with plant phytoconstituents profiling or metabolomics studies due to their high sensitivity and accuracy when coupled to influential chromatographic techniques [e.g., high-performance thin-layer chromatography (HPTLC), gas chromatography–mass spectrometry (GC–MS), capillary electrophoresis–mass spectrometry, and liquid chromatography–mass spectrometry] that allows the separation and characterization of the nonpolar and polar metabolites present in the medicinal plants.[7,8]

Furthermore, GC–MS is one of the advanced and the first choice of techniques due to its high selectivity, sensitivity, and enables extensive detection of nonpolar metabolites within a sample. It makes us far formalized to characterize a comprehensive matrix of metabolite or their accretion patterns without having liabilities on authentic reference compounds and or isolation of the individual metabolites. The structural assignment process generally depends on the reference database search to interpret for MS and MS–MS data. Moreover, unknown metabolite characterization is a little challenging, since these cannot be consigned to a reference database. Further, the fragmentation pattern–parent ions–daughter ions are the unique parameter in GC–MS–MS-based plant metabolomics which allows us far formalized for characterization of the targeted and untargeted metabolites based on *m/z* values and reference database.[9]

For authentication, the m/z values of metabolites are matched with the reference data of mass banks where the analysis is resumed under the defined tolerance of m/z values variability.[10] The MS data acquisition analysis depends on the probability score between query and reference data search. For the untargeted metabolites, the data acquisition tolerance can be both in m/z value and chromatographic retention time, and these implications are further accustomed across measurements by using alignment software.[11] Advanced web-based platform analyses have been established based on automated workflows from processing to peak alignment of row data, annotations, statistical analysis tools to enable easy access for a broad range of investigators, and informatics expertise.[12]

In the advent of the gradual rise of interdisciplinary subjects concerning bioinformatics and computational biology, researchers are being more prompted or have shifted for traditional medicine research from a single-mode to multi-faceted and dimensionalized systematic research mode. To understand the mechanisms of drug action are the significant changes from the perspective of the biomolecular network associated with the gene's role in disease regulation. The "network computational biology" aimed to regain or bring significant changes and resolve new challenges associated with the preliminary screening of the drugs.[13]

The network target represents unique concepts that characterize the biological network of therapeutic target underlying diseases and decipher systematic mechanisms of action for single multitargeted drugs, predominantly used for traditional medicine. Thus, the theory "network prediction of target" has been acknowledged as the core theory of network pharmacology.[14]

Traditional medicine (TM), characterized by personalized, multicomponent, and holistic therapy, grasps big potential to conceptualize various challenges in the system of modern health care. By producing an unprecedented prospect of TM for systematic research, network pharmacology is progressing as a systematic paradigm or even becoming a frontier research field of drug discovery and development.[15] The systematic perspective of network pharmacology is emphasized to reveal the systematic mechanisms of drug pharmacology and further implemented for the drug discovery and development or clinical treatment. Network pharmacology assimilates computational, experimental, and clinical investigation and generates promising aspects to explore the characteristics of TM and their further association with the frontiers of modern science and technology.[14]

T. cordifolia is a traditional Indian medicinal plant used for various ailments or chronic disorders in form of aqueous decoction. It has been part of various traditional formulations of AYUSH which are being used for centuries to cure urinary disorder/increased frequency and turbidity of urine, diabetes (API, Part-I, Vol-I, 41), and diuretic (UPI, Part-I, Vol-I,).[16]

Due to metabolite complexity, namely, fatty acids, steroids, terpenoids, alkaloids, and polyphenols, *T. cordifolia* is assisted in the regulation of chronic kidney malfunction via exertion of multidimensionality potential as antidiabetic and hypoglycemic activity, anti-inflammatory activity, anticancer activity, and immunomodulatory activity.[17,18] Although, no specific phytopharmacological evidence on *T. cordifolia* is still available which tends to identify an unknown nonpolar matrix of the phytoconstituents extracted with polar systems and establish based on their metabolic patterns and pharmacology related to kidney and associated diseases.

Several studies have been conducted on individual plant matrix of metabolites based on GC–MS and revealed the diversity of metabolites, such as lipid-related compounds, steroids, and organic acids, as well as

structurally diverse phytohormones. Further, the correlation of derived metabolites and target biological assessment has a vast consideration in the screening of the metabolites based on their biological interaction.[19]

Taking all these facts into consideration, the present study aimed to evaluate the comparative evaluation of the metabolomic pattern of different fractions obtained from *T. cordifolia*, and *in-silico* computational studies were performed to investigate the mechanism of screened constituents-based on network pharmacology hyphenated compound or protein–protein interaction (PPI) for nourishing kidney malfunction.

MATERIALS AND METHODS

Chemicals and reagents

The analytical-grade solvents such as *n*-hexane, dichloromethane, methanol, and distilled water used for sample preparation and GC–MS analysis were purchased from SD Fine-chem Limited, Mumbai.

Preparation of extract

Dried stem of *T. cordifolia* was provided as a gift sample to the bioactive natural product laboratory (BNPL) from AIMIL Pharmaceuticals (India) Ltd, Saini Majra, Ropar Nalagarh Rd, Tehsil Nalagarh, Solan District, H. *P* 174101, India, which was collected from Nalagarh district Solan, Himachal Pradesh, India and authenticated as per Ayurvedic Pharmacopoeia of India (API, Part-I, Vol-I, pg-53). The voucher specimen of each vendor was submitted to BNPL with voucher number BNPL/JH/Ph.D/11/19/04, BNPL/JH/Ph.D/11/19/05, and BNPL/JH/Ph.D/11/19/06. In brief, 100 g of the dried stem of *T. cordifolia* from each vendor was coarsely powdered using a grinder and soaked in 700 ml of distilled water overnight in three different round bottom flasks. Thereafter, the extraction process was performed using the reflux method at 60°C temperature for 8 hr. The extracts were filtered using a muslin cloth and Whatman™ filter paper (Qualitative, 90 mm; Cat No 1001090) and concentrated on a water bath at 60°C to get dried residue. The yields of extracts were calculated and stored in an air-tight container for further use.[20]

HPTLC profiling

HPTLC profiling of each aqueous extract of *T. cordifolia* was performed using the standard protocol with some modification in chromatographic condition while the instrument and instrumentation condition remained the same as followed in the protocol.[7] In brief, 30 mg of aqueous extract of each sample was dissolved in 1 ml of methanol followed by vortex and centrifugation for 10 min. The supernatant was collected for HPTLC analysis while toluene, ethyl acetate, and formic acid (5: 4: 1, v/v/v) were used as mobile phase to develop TLC plate (size 10 × 5 cm) in a presaturated TLC development chamber. After the development of TLC plate, fingerprinting analysis was performed at 254 nm.

Preparation of sample for GC–MS analysis

The aqueous extracts of different vendors as prepared in Section 2.2 were pooled in 1:1:1 ratio (w/w) and used for successive extraction/fractionation using hexane, dichloromethane (DCM), and methanol as extracting solvents. In brief, 60 mg of sample was taken in 1.5 ml Eppendorf's tube and directly dispersed in hexane, DCM, and methanol. Then, 1 ml of each solvent was added into Eppendorf's tube followed by vortex and centrifugation for repeated 10 min after completion of successive extraction with one solvent. Thus, all three fractions were obtained from mixed samples of *T. cordifolia* aqueous extract and processed for GC–MS metabolomic analysis in triplicate after filtering through a 0.2 µM polytetrafluoroethylene membrane filter.

GC–MS Metabolomics analysis

The study was performed on a GC–MS instrument (Agilent 7890A, Agilent Technologies, United States) equipped CTC-PAL autosampler associated with a mass spectrophotometer detector (Agilent 5975C inert XL EI/CI MSD with Triple-Axis Detector, Agilent Technologies, United States). In brief, 2.0 µL of each prepared sample was injected with a 10:1 split ratio onto a 30 m × 0.25 mm × 0.25 µm HP-5MS column (5% diphenyl, 95% dimethyl polysiloxane, Agilent Technologies, United States). The oven temperature was set at 50°C initially for 1 min and further gradually increased up to 150°C at 5°C/min, and the temperature was held for 1 min. Then, it was ramped to 310°C at 10°C/min; 310°C was maintained for 5 min. The total run time of the sample run was 41 min. The chromatographic separation was done using high pure helium (99.999%) as carrier gas at a constant flow rate of 1 mL/min. The injection port, transfer line, and ion source temperatures were all set at 250°C while 70 eV of EI was adopted, and the mass scanning range was set from 50 to 700 amu in full scan. Solvent interruption time was adjusted at 3 min for all samples generated by different methods. To process chromatographic and spectral data, MSD ChemStation software was used. The metabolites separated through GC–MS were identified by comparing the obtained mass spectra of the analytes with those of authentic standards from the NIST libraries (2005) and with the mass spectra published previously.[9] The analysis of each sample was done in triplicate (n = 3).

Data processing based on metabolites pattern obtained from the different fractions of *T. cordifolia* aqueous extract

The metabolites identified from GC–MS analysis were formatted as per the presence (value 1) or absence (value 0) of metabolite in different fractions of mixed samples. The formatted data were further analyzed by the XLSTAT2021.lnk trial version for principal component analysis (PCA) and multivariate data analysis. The Extended Statistics module of the XLSTAT software was used to implement multivariate statistical analysis for the data obtained by GC–MS profiling of different fractions of *T. cordifolia* aqueous extracts. Partial least squares discriminate analysis with Pareto scaling was used to evaluate comparative metabolites variability and identify metabolite variables that are responsible for potential metabolites among different samples. Further, the metabolites network/matrix was evaluated between three successive fractions and their identified metabolite content. To determine the distance between different generated clusters of each fraction metabolites, the Ward distance algorithm was used to calculate through hierarchical cluster analysis (HCA). Using the PCA-to-HCA, 40 metabolomic tree diagrams were created, and the corresponding bootstrap values were calculated to interpret the PCA clustering pattern.[21]

ADME analysis

ADME computational analysis was performed for each metabolite identified in different fractions of *T. cordifolia* mix sample through "SwissADME (http://www.swissadme.ch/index.php)." Topological polar surface area (TPSA) for drug integrity, consensus log Po/w for drug lipophilicity, log K_p (skin permeation), and drug-likeness were predicted as the standard parameters for their bioavailable or ADME response, and to determine the relationship of ADME analysis between each parameter.[22]

Gene ontology and network pharmacology analysis

Genes involved in kidney and associated disorders were selected from Genecard (https://www.genecards.org/) and UniPort database (https://

www.uniprot.org/uploadlists/) with their UniPort ID.[23] Gene ontology (GO) analysis through Metascape (metascape.org) tool was performed to evaluate multiple physiological roles of each gene in the regulation of kidney and associated disorders after the analysis of the compound-disease common target. A PPI and compound–proteins interaction network was constructed and integrated using STRING platform (https://string-db.org/) and Cytoscape (version 3.8.2) software. The analysis covered all the nearly functional interactions among the expressed proteins–proteins and compound–proteins.

RESULTS AND DISCUSSION

The extraction process of three different vendors of *T. cordifolia* using distilled water was done successfully. The average extractive yield of aqueous extract was found to be 13.74% ± 1.632%, which was within the limit of India's Ayurvedic pharmacopeia (API, Part-I, Vol-I, p-65). After the successful extraction of *T. cordifolia* aqueous extracts, HPTLC analysis was performed to determine the variability among samples, if any. Thereafter, GC–MS analysis was performed on hexane, DCM, and methanol fractions in triplicate, which was obtained by successive extraction from pooled samples of aqueous extracts.

HPTLC analysis

HPTLC analysis of each aqueous extract of *T. cordifolia* was performed to determine the variability among samples. The fingerprinting analysis showed several major and minor metabolites in each extract of *T. cordifolia* at different Rf scale: 0.076, 0.123, 0.171, 0.219, 0.276, 0.352, 0.380, 0.457, 0.504, 0.742, 0.780, and 0.819 for TCS1; 0.075, 0.123, 0.170, 0.217, 0.274, 0.350, 0.378, 0.455, 0.502, 0.741, 0.780, and 0.818 for TCS2; and 0.075, 0.123, 0.170, 0.218, 0.274, 0.351, 0.380, 0.455, 0.504, 0.741, 0.780, and 0.819 for TCS3. The resulted data showed no significant differences in the number of metabolites and their respective peak intensity in aqueous extract of tested vendors of *T. cordifolia*. Considering these facts, the HPTLC analysis of different vendors of *T. cordifolia* can be assessed potentially in quality-based standardization of its herbal medicine or products.[24] Since no significant differences were observed in intensities of peaks commonly present at different R_f it was decided to pool the samples in 1:1:1 ratio (w/w/w) for further analysis.

GC–MS analysis

The comparative metabolomic analysis of each fraction obtained from mixed extracts of *T. cordifolia* from different vendors was done

Table 1: Phytochemical screening from different fractions of *T. cordifolia* using GC–MS analysis

Identified Compound	Molecular Weight	Retention Time (Rt)	Hexane Fraction	DCM Fraction	Methanolic Fraction
(14β)-Pregnane	288.5	26.437	+	–	+
2 (1H)-Naphthalenone	152.23	12.291	+	–	–
6-Aza-5,7,12,14-Tetrathiapentacene	355.5	9.083	–	–	+
6-Methyloctahydrocoumarin	168.23	13.352	+	–	–
7-Pentadecyne	208.38	23.932	–	+	–
Anisole	108.14	13.954	+	+	–
Anthracene	178.23	18.727	+	–	–
Artonin L Monomethyl Ether	272.25	30.295	–	–	+
Bisphenol A	228.29	27.696	+	–	+
Camphene	136.24	10.665	–	–	+
Capric Acid	172.26	6.008	–	–	+
Cinnamaldehyde	132.16	11.86	–	–	+
Citronellal	154.25	19.100	–	+	–
Curcumene	368.38	14.582	–	–	+
Cyercene 4	262.34	22.710	–	–	+
D-Allose	180.15	6.404	–	–	+
Diethyl Phthalate	222.24	15.995	+	+	+
Docosane	310.60	20.411	–	–	+
Eicosene	280.53	21.589	+	+	+
Erucic Acid	338.57	30.888	–	–	+
Ethyl Caprylate	172.26	10.467	+	–	+
Eugenol	164.27	13.045	–	–	+
Fukinanolid	234.33	22.702	–	–	+
Fulvic acids	308.24	6.118	+	–	–
Fumaric Acid	116.07	13.264	+	+	–
Heneicosanoic Acid	326.56	9.472	+	+	+
Lauric Acid	200.31	6.118	–	–	+
Linoleic Acid	280.44	24.306	+	+	+
Methyl Linoleate	294.53	28.889	+	+	+
Methyl Palmitate	270.45	20.564	+	–	+
Morpholine	87.1	5.503	–	+	+
Myristylaldehyde	212.37	14.648	+	–	–
Oleic Acid	282.47	26.656	+	+	+
Palmitic Acid	256.4	20.557	+	–	+
Phthalic Acid	166.14	19.627	+	+	+
Vaccenic Acid	282.46	26.627	+	+	+
Valencene	204.35	14.897	–	+	–
Vibrindole A	260.33	21.194	–	–	+
Vitamin E	260.33	31.562	+	–	+
Zingiberene	204.18	14.736	–	–	+
Total metabolites			20	14	30

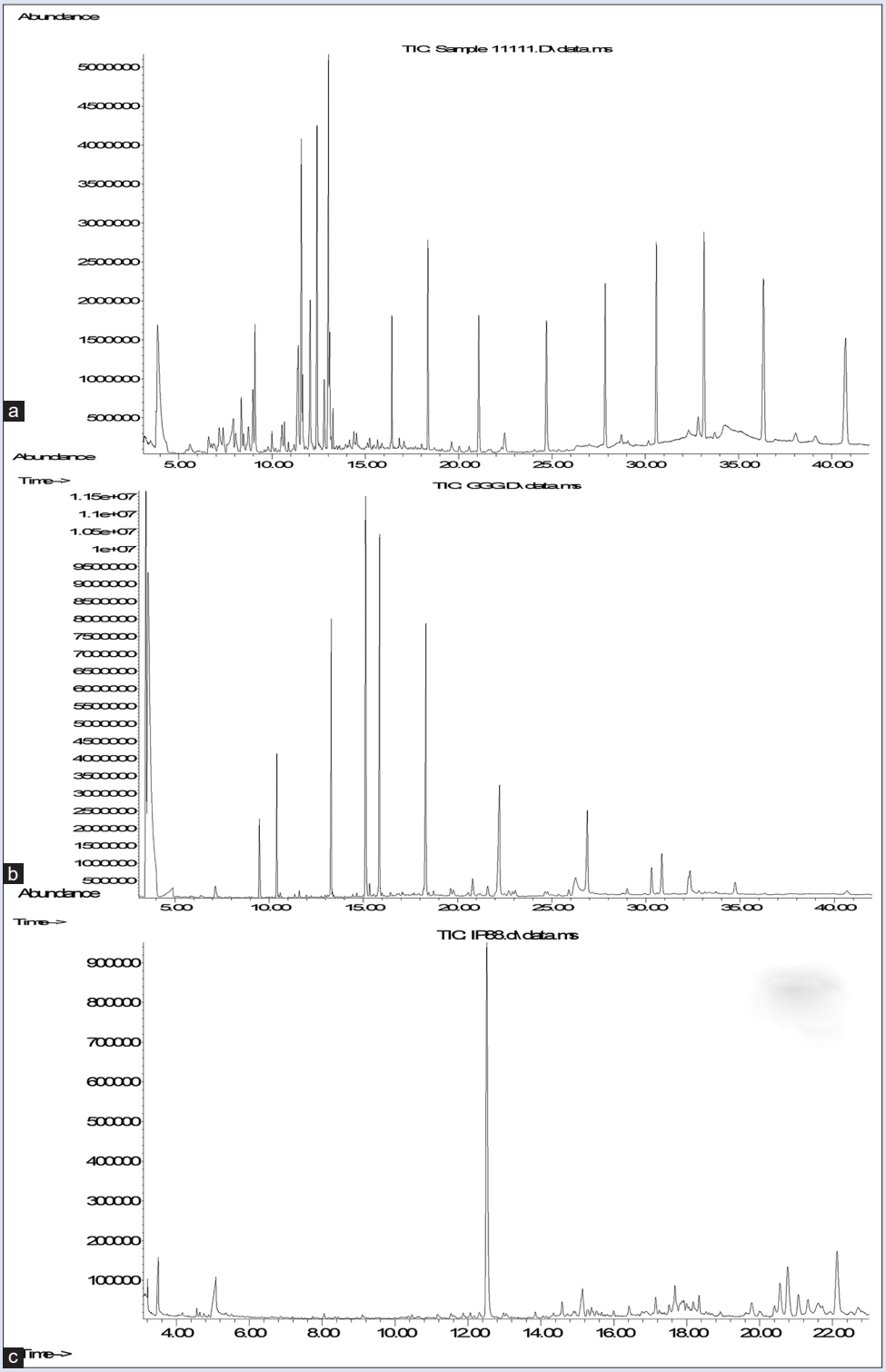

Figure 1: GC–MS chromatogram of different samples. (a) Represents the chromatogram of hexane fraction. (b) Represents the chromatogram of DCM fraction. (c) Represents the chromatogram of methanolic fraction obtained from *T. cordifolia* aqueous extract

successively using the GC–MS instrument (Agilent 7890A, Agilent Technologies, United States). In GC–MS analysis, 40 metabolites were identified in the entire fractions. Meanwhile, 20 metabolites were identified in hexane fraction, 13 in DCM fraction, and 31 in the methanolic fraction of *T. cordifolia* aqueous extract. The compounds which were not of choice were removed during the processes of data acquisition. The screened metabolites were lipids/fatty acids, anthracenes, terpenes (monoterpenes and/or sesquiterpene), steroids, phenols, and alkaloids. The previous findings strongly support our findings.[16,25] In the analysis, some of the common metabolites were identified in each fraction and the principal metabolites matrix evaluations were done by comparative metabolites variability and

identify metabolite variables analysis which acknowledges the potential metabolites in each fractionated matrix of *T. cordifolia* aqueous extract. The identified metabolites in each fraction of *T. cordifolia* aqueous extract are summarized in Table 1 with their respective chromatograms presented in Figure 1.

Data processing based on metabolites pattern obtained from the different fractions of *T. cordifolia* aqueous extract

PCA was performed to identify the major differentiating metabolites present in different fractions of aqueous extract of *T. cordifolia*. Metabolites identified from GC associated with EI–CI MSD with triple-axis were matched with the authentic standards from the NIST libraries of metabolites. The data were formatted as per the presence (value 1) or absence (value 0) of metabolite in different fractions of *T. cordifolia* aqueous extract [Table 1]. PCA was performed among the assigned 40 metabolites converted to two main components on the x-axis (PC1) and y-axis (PC2). The statistical values were optimized and set at the significance level alpha = 0.05 for the PCA. Correlation matrix [Pearson (n)] and Eigenvalues of covariance were determined to represent matrix "core," directions of the new feature space, and their magnitude of the PCA. Generally, PCA is used to determine the general interrelation among the metabolite patterns of different fractions of plant matrix.[21] We specifically presented a deep analysis by the different ways for investigating the analytical data of major abundant and principal metabolites which differentiate each fraction of *T. cordifolia* aqueous extract. The statistical analysis revealed each centering and scaling variable to unit variance. The cumulative percentage variability of F1 (hexane fraction), F2 (DCM fraction), and F3 (methanolic fraction) components were 50.795%, 28.667%, and 20.538%, respectively. Further, the most prominent clustering in the square graph postulates that the fraction analysis of *T. cordifolia* aqueous extract merely had high dissimilarity among the metabolites of each fraction. The active variable PCA biplot axis graph showed hexane and DCM fraction with less dissimilarity of metabolites than a methanolic fraction. The contribution of the variables represents the highly contributed variables in the PCA and can be measured to determine the variables which are intensely influencing a particular PC. Additionally, when inferring the squared cosine between the variables and the PC, real correlations exist can be determined for their apparent relation.[26] The analysis reveals that the contribution and squared cosines of the variables are proportionated together with high contribution variability 51.67% by the F3 variables while 0.611 and 0.590 squared cosines for F1 and F2 variables with 0.676 squared cosines for F3 variable showed the largest squared cosine. Due to high variables and dissimilarity of metabolites in methanolic fraction, high contribution percent variability and squared cosines were determined. Further, in correlation analysis of eigenvalue, variability (%), and cumulative %, it has been observed that percentage variability is irreversibly proportionated to the cumulative % of the variables which depends on the dissimilarity of metabolite among each variable. In F3, the large set of metabolites variability can differentiate another's components, while F2 has the same

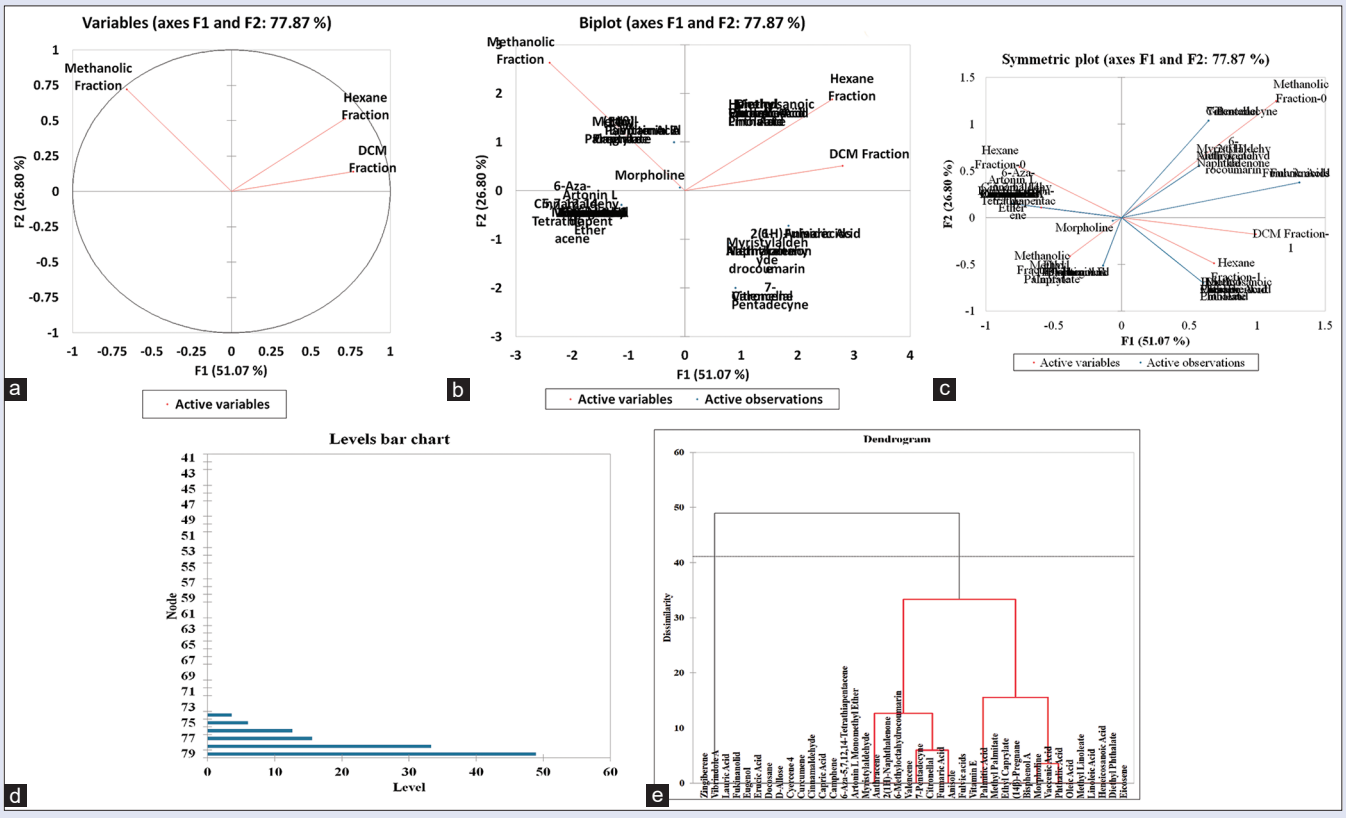

Figure 2: Representation of PCA. (a) Represents the squire plot of PCA; the samples in the same quadrant have similar metabolite patterns while the sample appeared in different quadrant has different metabolites pattern. (b) Represents Biplot of variables based on metabolite variation and showing active variables and observations corresponding to active observations, while (c) represents a symmetric plot of MCA that showed correlative pattern of metabolites with respect to each variable. In the dissimilarity index of agglomerative hierarchical clustering analysis of different variables, (d) represents the node variability bar graph, while (e) represents the dendrogram clustering targets of metabolites variability

correlation matrix considered as F1even no differentiation was observed in the eigenvalue for both the components. Based on this observation, PC1 acknowledged the correlation analysis for another component.

In multiple correspondence analysis (MCA), it has been observed that the samples that fall in the same compartment have similar metabolites patterns while the degree of rotation of active observations concerning the corresponding compartment is characterized by the different levels of variability. In symmetric plot analysis (axes F1 and F2: 77.87%), the observation revealed that hexane and DCM fraction metabolites have almost the same metabolites pattern while the large difference was observed in the F3 variable. Square variable plot and biplot for active variable and observation represented for PCA while symmetric plot represented for MCA is shown in Figure 2.

Besides the representation of data based on dissimilarity, is one of the simple statistical analytical methods with high applicability on various data sets. Dissimilarity index agglomerative hierarchical clustering (AHC) analysis was performed to determine relatively homogeneous clusters of a data set based on their characteristics measured in each variable. The output of dissimilarity dendrogram statistical analysis of GC–MS data is depicted with the four clusters of the data set. The first right cluster of metabolites showed the dissimilarity index of metabolites from hexane fraction, the second cluster showed for DCM fraction, the third-largest cluster showed for the common metabolites for hexane and methanolic fraction, while the remaining one set of the cluster showed for the common metabolites for each variable. Dissimilarity index AHC analysis node and dendrogram plot are shown in Figure 2.

ADME analysis

ADME profiling of identified metabolites from subfractions of mix *T. cordifolia* extract was determined based on TPSA, lipophilicity, permeability, and drug-likeness parameters. The comparative analysis of each corresponding parameter to determine the relationship of metabolites in the ADME process revealed that the molecules that have high TPSA value showed less permeability or even to the blood–brain barrier (BBB). Besides, those molecules having low TPSA value showed high permeability to the skin and BBB. The statistical representation of correlation analysis between consensus log P and log Kp (cm/s) revealed that the permeability of each metabolite is directly proportional to the lipophilicity of metabolites. The correlation coefficient was found to be 0.9483, 0.9802, and 0.9656 for hexane, DCM, and methanolic subfraction metabolites ADME parameters. Further, the correlation analysis was performed between TPSA and other parameters, the statistical analysis suggested no significant correlation of TPSA to consensus log P and log Kp (cm/s). It can be suggested that molecular integrity and permeability do not correlate with TPSA to predict the ability for permeation into BBB. The generated computational *in-silico* data and correlation plot of all the subfraction/metabolites for ADME applicability are shown in Figure 3 and the results of ADME analysis of each metabolite identified in different fractions are summarized in supplementary files named ADME_HF for identified metabolites in hexane fraction, ADME_DCMF for identified metabolites in DCM fraction, and ADME_MF for identified metabolites in methanolic fraction.

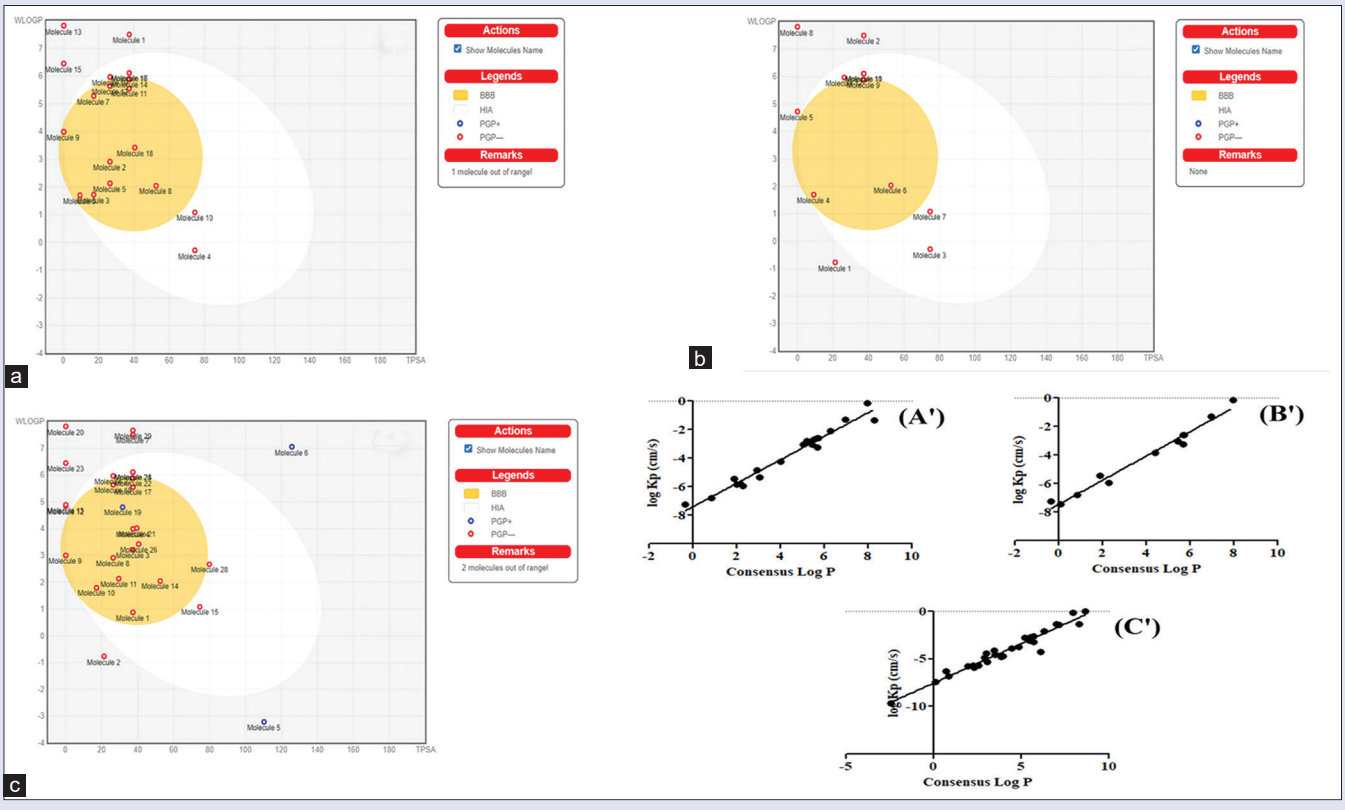

Figure 3: ADME analysis of each metabolite of different fraction. (a) Represents boiled egg plot for pharmacokinetics of hexane fraction metabolites. (b) Represents boiled egg plot for pharmacokinetics of DCM fraction metabolites, while (c) represents boiled egg plot for pharmacokinetics of methanolic fraction metabolites. Further correlation analysis was performed on lipophilicity and permeability strength of each metabolite, and the results were represented graphically in terms of log Kp (cm/s) and consensus log P. (A') Represents the relationship among hexane fraction metabolites, (B') for DCM fraction, and (C') for methanolic fraction

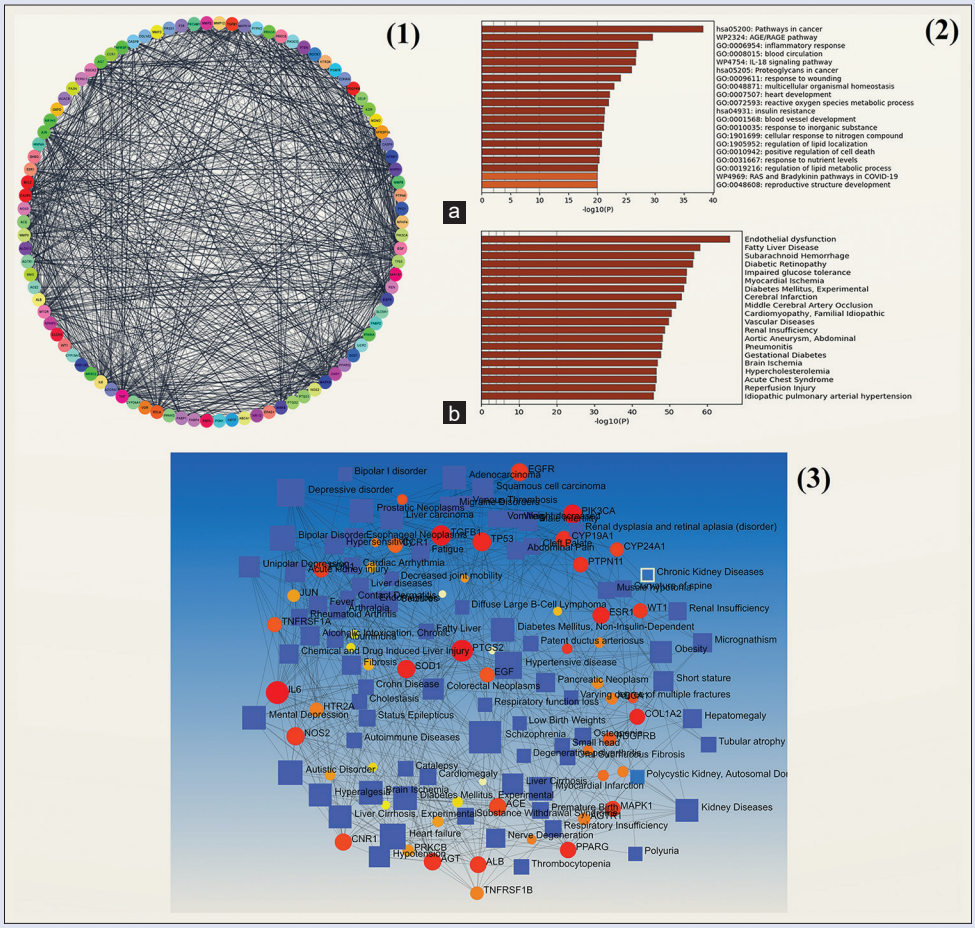

Figure 4: GO analysis of target genes. (1) Common network establishment of protein–protein interaction. (2a) Represents GO analysis of target genes which represents a bar graph of enriched terms across input gene lists and colored by *P* values, while (2b) represents summary of enrichment analysis in DisGeNET. (3) Represents the gene-disease association of targeted genes

Gene ontology and network pharmacology analysis

In this analysis, a set of 100 target genes were selected from different gene databases. The selection of each target gene was constrained to kidney and associated diseases only. The target genes which had less even no significant interaction with metabolites were excluded during the integration analysis. The set of 93 genes is summarized.

Common target network (protein-protein interaction)

In this analysis, ninety-three putative target genes were found interconnecting each other. A PPI network was constructed using STRING database with a medium confidence score of 0.400. The established network embodied 93 nodes, 1006 edges, 21.4 average nodes of degree, and 0.599 average coefficients of local clustering. Besides, the established protein–protein network has significantly more interactions than expected. The significant interaction of each protein–target gene is based on proteins of similar size selected from the genome database and characterized that the proteins are at least partially biologically connected to each other during kidney dysfunction or associated factors. The edges characterize the interaction between sets of potential targets, while the nodes characterize the targets [Figure 4].

Further, the target genes were analyzed for gene ontology through Metascape Gene Analysis (metascape.org) and gene-disease association through network analysts to evaluate the multiple physiological roles of each gene in the regulation of kidney and associated disorders. Out of 96 genes, the top 20 results were selected which were directly interrelated with the pathophysiology of the kidney. The observation of enriched terms across input gene and enrichment analysis in DisGeNET revealed that many targeted genes play a vital role in managing kidney and associated disease via preventing renal insufficiency, reactive oxygen species, diabetic nephropathy, hypertension/vascular disease, and inflammation and various apoptotic pathways.[23] The bar graph of enriched terms across input gene lists, colored by *P* values and the summary of enrichment analysis in DisGeNET and gene-disease association network is summarized in Figure 4.

Network construction for active components common targets

In the network establishment analysis of compound and disease common targets, 40 metabolites obtained from GC–MS analysis of each fraction of *T. cordifolia* were analyzed based on their significant interaction with the target gene. A compound-disease common target network was established using Cytoscape 3.8.2 and analyzed or interpreted for their significant interaction. The screening of potential metabolites was done based on the degree of interaction, interacted nodes, and number of interrelated edges with neighbor nodes. The metabolites which had no interaction with the target gene/node were deleted during interpretation analysis of the network. The observation revealed

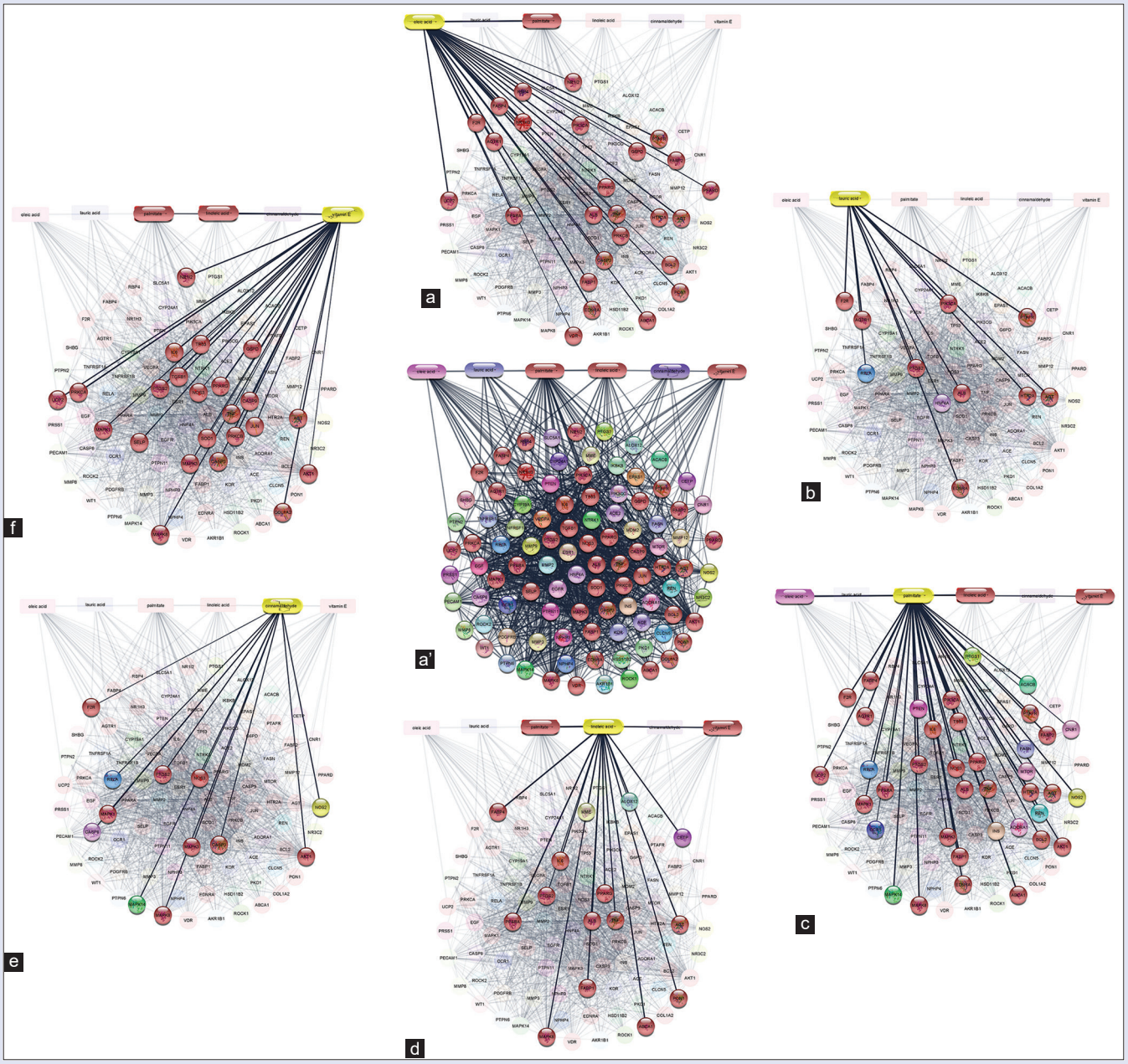

Figure 5: Network pharmacological analysis of potential metabolites with target genes. (a) Represents enrichment gene interaction of oleic acid. (b) Represents enrichment gene interaction of lauric acid. (c) Represents enrichment gene interaction of methyl palmitate. (d) Represents enrichment gene interaction of linoleic acid. (e) Represents enrichment gene interaction of cinnamaldehyde. (f) Represents enrichment gene interaction of vitamin E, while the figure embedded in the center represents common target interaction of each metabolites

that out of 40 metabolites, only six metabolites were identified as four fatty acids, namely, oleic acid, lauric acid, palmitate, linoleic acid, one aldehyde; cinnamaldehyde and vitamin E have significant interaction with each target used in analysis which may suggest their strong biological connection in management of kidney and associated disorders [Figures 5 and 6]. During interpretation analysis, oleic acid showed interaction with 25 genes, such as UCP2, AGTR1, PPARG, HTR2A, CASP3, PIK3CA, TNF, BCL2, and FABP2, which could play a pivotal role in the regulation of arterial blood pressure, ion transportation/calcium homeostasis, management of diabetes and diabetic nephropathy, tumor suppression (bladder tumor), and oxidative modification. TNF signaling is well acknowledged with inflammatory cytokine associated with renal injury. TNF-α, NF-κB triggers the activation and transcription of ICAM-1, IL-6, and IL-8, which results in endothelial inflammatory and acceleration of renal pathogenesis.[27,28] Oleic acid nitration is facilitated for regulation of many reactive nitrogen oxides such as the nitrogen dioxide radical and demonstrated benefits in hypertension, hyperglycemia in diabetes, obesity with the metabolic syndrome, and vascular neointimal proliferation and turns the nonselective activation of PPAR, which may in part account for OA-NO2's biological effects. Further, it has been reported that oleic acid acts as a strong candidate against inflammation via the prosurvival nrf2-signaling pathway.[29,30] In a report of Perdomo *et al.*,[31] Oleate reduces pro-inflammatory cytokines induced eNOS expression, impaired the proliferation induced by TNF-α, angiotensin II and the apoptosis induced by TNF-α or thapsigargin in endothelial cells (ECs) and vascular smooth muscle cells (VSMCs).

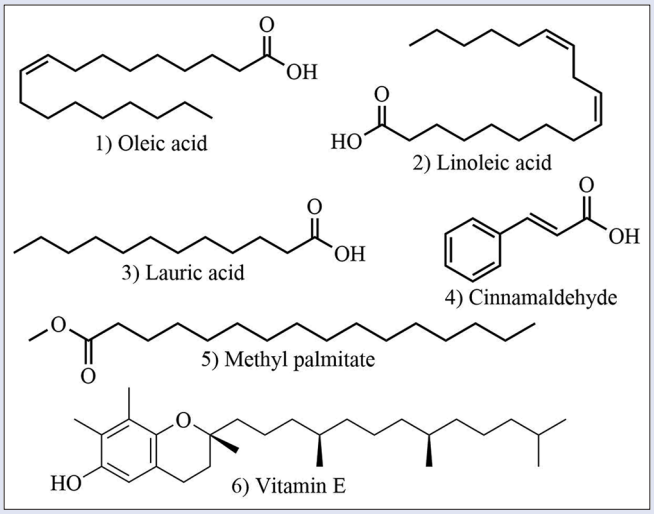

Figure 6: Chemical structures of potential metabolites have significant interaction with target genes

Lauric acid showed 11 interrelated edges genes, such as PTAFR, ALB, HNF4A, and PIK3CA, who regulate colloidal osmotic pressure of blood, smooth muscle contractile and hypotensive activity, vascular development, resistance to apoptosis, and tumor angiogenesis. Further, it strongly regulates blood pressure and increases sodium retention by the kidney. Moreover, HNF4A plays a critical role in proximal tubule development and is responsible for mechanistic insight into the etiology of Fanconi renotubular syndrome with major symptoms such as excess excretion of glucose, water, phosphate through urination, polyuria, polydipsia, glycosuria, and phosphaturia.[32]

Phosphatidylinositol 4,5-bisphosphate 3-kinase catalytic subunit alpha isoform of phosphoinositide-3-kinase (PI3K) protein member families are well-known regulators of proliferative signals. It activates AKT/PKB and mammalian target of rapamycin (mTOR) pathways by the generation of lipid second messengers. The variations in the proliferative signals lead to overgrowth disorders and polycystic kidney disease through alterations in PI3K enzymes at different signaling cascades.[33] In diabetes, increase evidence of proteinuria ≥300 mg/day, vascular injury, hypertension, and significant glomerular damage are the sensitive and early indicators of tubule damage due to diabetes-induced oxidative and inflammatory stress by altering the function of genes such as INS, TNF, IL6, MAPK1, mTOR, and NOS3.[34–36] The renin-angiotensin system (RAS) or associated genes such as AGTR1 and AGT play an essential role in the management of kidney malfunction. If the RAS is overactive, it promotes arterial constriction, resulting in an increase in blood pressure, electrolyte disbalance, and decrease in renal function.[37,38] Our findings suggest that the methyl palmitate, linoleic acid, and cinnamaldehyde have significant interaction with the defined target gene and can be a key regulator against the deleterious effect of vascular distortion, oxidative, and inflammatory stress.

Cinnamaldehyde is a phenylpropanoid phytoconstituents reported for reno-protective action via attenuation of oxidative and inflammatory stress.[39] In the cited study, it has been reported that cinnamaldehyde acts as a key regulator for interleukin's, TNF's, and p38 mitogen-activated protein kinase (MAPK), thereby improving signaling pathways involved in inflammations or even apoptosis.[40] It has further been documented to inhibit lipid peroxidation induced TLR-4 dimerization by cysteine residues modification into PI3K and phosphoinositide-dependent kinase-1 (PDK-1) and regulate upstream monocyte/macrophage-mediated immune responses via NF-κB signaling.

In a recent study, it was emphasized that vitamin deficiency leads serious harm to the kidney and is progressive to end-stage renal disease (ESRD). Moreover, cardiovascular risk in patients with mild-to-moderate renal insufficiency may lead to high morbidity and mortality. Vitamin E is a fat-soluble vitamin with potent antioxidants with anti-inflammatory properties, it predominantly hinders lipid peroxidation that occurs in the cell membrane and suppresses free radicals-induced inflammatory stress.[41]

In a recent study, vitamin E, its molecular mechanisms and signaling pathways linked to malignancy modulated by its vitamers and inflammation. Preclinical reports emphasized a myriad of cellular effects via modulation in pro-inflammatory molecules and oxidative stress response, thus inhibiting the NF-κB pathway, regulating cell cycle, and apoptosis. Furthermore, it regulates various molecular effects including enzyme activity and signaling pathways, such as SOD, CAT, GPx, MAPK, PI3K/Akt/mTOR, JAK/STAT, and NF-κB, acting as the underlying mechanisms of their reported antioxidant and anti-inflammatory effects. In clinical settings, it has been proven that vitamin E potentially improves redox and inflammatory status in healthy, diabetic, and metabolic syndrome subjects.[42]

Therefore, the results of network pharmacological analyses not only validate the screened targets but also represent the fatty acids whether isolated from any sources have a significant therapeutic role in the kidney or associated disease by regulating several pathophysiological pathways, including hypertension, oxidative/inflammatory stress, insulin resistance, apoptosis, and other pathways with unclear mechanisms. The significant interaction of each target with fatty acids will provide a novel methodology for further assessment of a therapeutic/mechanical approach to alleviating kidney disease.

CONCLUSION

The study found that *T. cordifolia* aqueous extract possesses several major and minor nonpolar metabolites identified by GC–MS analysis. PCA statistical analysis reveals the high variability among each variable especially in methanolic fraction with a large difference in eigenvalue than other variables. Further, based on network pharmacology analysis, it was investigated that four fatty acids such as oleic acid, lauric acid, palmitate, linoleic acid, one aldehyde; cinnamaldehyde, and vitamin E have significant interaction with the targets associated with kidney disorders. The analysis can enlighten the role of screened fatty acids and other metabolites in treating kidney disease and related disorders via ameliorating hypertension, oxidative/inflammatory stress, insulin resistance, and apoptosis kind of pathophysiological conditions. Besides, the generated evidence can be the best source to explore the therapeutic or mechanistic approaches for *T. cordifolia* to alleviate chronic kidney disease, practically.

Acknowledgements

The authors would like to thank the Ministry of AYUSH for providing the facilities at the Centre of Excellence in Unani Medicine (Pharmacognosy and Pharmacology), Jamia Hamdard, New Delhi, India and AIMIL pharmaceuticals for providing the raw material of plant samples required for testing.

Authorship contribution statement

Gaurav: Investigation, writing, drafting, software, and visualization; **Mohammad Umar Khan:** formal analysis; **Sultan Zahiruddin:** GC–MS analysis and data acquisition; **Parakh Basist:** software and visualization;

Gaurav and Rabea Parveen: data curation and validation; **Rabea Parveen and Anuja Krishnan:** supervision, writing, review, and editing; **Sayeed Ahmad:** conceptualization, resources, writing, review, and editing original draft.

Financial support and sponsorship

Nil.

Conflicts of interest

There are no conflicts of interest.

REFERENCES

1. Zhou B, Xiao JF, Tuli L, Ressom HW. LC-MS-based metabolomics. Mol Biosyst 2012;8:470-81.
2. Khoo SHG, Al-Rubeai M. Metabolomics as a complementary tool in cell culture. Biotechnol Appl Biochem 2007;47:71-84.
3. Goodacre R, Vaidyanathan S, Dunn WB, Harrigan GG, Kell DB. Metabolomics by numbers: Acquiring and understanding global metabolite data. Trends Biotechnol 2004;22:245-52.
4. Salem MA, De Souza LP, Serag A, Fernie AR, Farag MA, Ezzat SM, *et al.* Metabolomics in the context of plant natural products research: From sample preparation to metabolite analysis. Metabolites 2020;10. doi: 10.3390/metabo10010037.
5. Senguttuvan J, Paulsamy S, Karthika K. Phytochemical analysis and evaluation of leaf and root parts of the medicinal herb, Hypochaeris radicata L. for *in vitro* antioxidant activities. Asian Pac J Trop Biomed 2014;4(Suppl 1):S359-67.
6. Gad HA, El-Ahmady SH, Abou-Shoer MI, Al-Azizi MM. Application of chemometrics in authentication of herbal medicines: A review. Phytochem Anal 2013;24:1-24.
7. Gaurav, Zahiruddin S, Parveen B, Ibrahim M, Sharma I, Sharma S, *et al.* TLC-MS bioautography-based identification of free-radical scavenging, α-amylase, and α-glucosidase inhibitor compounds of antidiabetic tablet BGR-34. ACS Omega 2020;5:29688-97.
8. Jorge TF, Mata AT, António C. Mass spectrometry as a quantitative tool in plant metabolomics. Philos Trans R Soc A Math Phys Eng Sci 2016;374. doi: 10.1098/rsta.2015.0370.
9. Khan W, Parveen R, Chester K, Parveen S, Ahmad S. Hypoglycemic potential of aqueous extract of Moringa oleifera leaf and *in vivo* GC-MS metabolomics. Front Pharmacol 2017;8:577.
10. Smith CA, Want EJ, O'Maille G, Abagyan R, Siuzdak G. XCMS: Processing mass spectrometry data for metabolite profiling using nonlinear peak alignment, matching, and identification. Anal Chem 2006;78:779-87.
11. Pluskal T, Castillo S, Villar-Briones A, Orešič M. MZmine 2: Modular framework for processing, visualizing, and analyzing mass spectrometry-based molecular profile data. BMC Bioinformatics 2010;11:395.
12. Sawada Y, Yokota Hirai M. Integrated LC-MS/MS system for plant metabolomics. Comput Struct Biotechnol J 2013;4:e201301011.
13. Yi F, Li L, Xu L-jia, Meng H, Dong Y-mao, Liu H-bo, *et al. In silico* approach in reveal traditional medicine plants pharmacological material basis. Chinese Med (United Kingdom) 2018;13:33.
14. Lai X, Wang X, Hu Y, Su S, Li W, Li S. Editorial: Network pharmacology and traditional medicine. Front Pharmacol 2020;11:1194. doi: 10.3389/fphar.2020.01194.
15. Yang M, Chen J, Xu L, Shi X, Zhou X, An R, *et al.* A network pharmacology approach to uncover the molecular mechanisms of herbal formula Ban-Xia-Xie-Xin-Tang. Evidence-based Complement Altern Med 2018;2018:4050714. doi: 10.1155/2018/4050714.
16. Upadhyay A, Kumar K, Kumar A, Mishra H. *Tinospora cordifolia* (Willd.) Hook. f. and Thoms. (Guduchi)-validation of the Ayurvedic pharmacology through experimental and clinical studies. Int J Ayurveda Res 2010;1:112-21.
17. Ghosh S, Saha S. *Tinospora cordifolia*: One plant, many roles. Anc Sci Life 2012;31:151-9.
18. Sharma P, Dwivedee BP, Bisht D, Dash AK, Kumar D. The chemical constituents and diverse pharmacological importance of *Tinospora cordifolia*. Heliyon 2019;5:e02437.
19. Fernie AR. Metabolome characterisation in plant system analysis. Funct Plant Biol 2003;30:111-20.
20. Parveen A, Zahiruddin S, Agarwal N, Akhtar Siddiqui M, Husain Ansari S, Ahmad S. Modulating effects of the synergistic combination of extracts of herbal drugs on cyclophosphamide-induced immunosuppressed mice. Saudi J Biol Sci 2021;28:6178-90.
21. Khan J, Sheoran S, Khan W, Panda BP. Metabolic differentiation and quantification of gymnemic acid in *Gymnema sylvestre* (Retz.) R.Br. ex Sm. leaf extract and its fermented products. Phytochem Anal 2020;31:488-500.
22. Daina A, Michielin O, Zoete V. SwissADME: A free web tool to evaluate pharmacokinetics, drug-likeness and medicinal chemistry friendliness of small molecules. Sci Rep 2017;7:42717. doi: 10.1038/srep42717.
23. Li Y, Wang L, Xu B, Zhao L, Li L, Xu K, *et al.* Based on network pharmacology tools to investigate the molecular mechanism of cordyceps sinensis on the treatment of diabetic nephropathy. J Diabetes Res 2021;2021:8891093. doi: 10.1155/2021/8891093.
24. Attimarad M, Mueen Ahmed KK, Aldhubaib BE, Harsha S. High-performance thin layer chromatography: A powerful analytical technique in pharmaceutical drug discovery. Pharm Methods 2011;2:71-5.
25. Sinha A. Phyto-chemical studies of methanol extracts of *Tinospora cordifolia* stem by GC-MS. World J Pharm Res 2017;1319-26.
26. David CC, Jacobs DJ. Principal component analysis: A method for determining the essential dynamics of proteins. Methods Mol Biol 2014;1084:193-226.
27. Ramseyer VD, Garvin JL. Tumor necrosis factor-α: Regulation of renal function and blood pressure. Am J Physiol Ren Physiol 2013;304:F1231-42.
28. Su H, Lei CT, Zhang C. Interleukin-6 signaling pathway and its role in kidney disease: An update. Front Immunol 2017;8:405.
29. Menon MC, Chuang PY, He JC. Nitro-oleic acid is a novel anti-oxidative therapy for diabetic kidney disease. Am J Physiol Ren Physiol 2013;305:F1542-3.
30. Szczuko M, Kaczkan M, Drozd A, Maciejewska D, Palma J, Owczarzak A, *et al.* Comparison of fatty acid profiles in a group of female patients with chronic kidney diseases (CKD) and metabolic syndrome (MetS)–similar trends of changes, different pathophysiology. Int J Mol Sci 2019;20. doi: 10.3390/ijms20071719.
31. Perdomo L, Beneit N, Otero YF, Escribano Ó, Díaz-Castroverde S, Gómez-Hernández A, *et al.* Protective role of oleic acid against cardiovascular insulin resistance and in the early and late cellular atherosclerotic process. Cardiovasc Diabetol 2015;14:75.
32. Marable SS, Chung E, Adam M, Potter SS, Park JS. Hnf4a deletion in the mouse kidney phenocopies Fanconi renotubular syndrome. JCI Insight 2018;3. doi: 10.1172/jci.insight.97497.
33. De Santis MC, Sala V, Martini M, Ferrero GB, Hirsch E. PI3K signaling in tissue hyper-proliferation: From overgrowth syndromes to kidney cysts. Cancers (Basel) 2017;9. doi: 10.3390/cancers9040030.
34. Sulaiman MK. Diabetic nephropathy: Recent advances in pathophysiology and challenges in dietary management. Diabetol Metab Syndr 2019;11:7.
35. Giacco F, Brownlee M. Oxidative stress and diabetic complications. Circ Res 2010;107:1058-70.
36. Gödel M, Hartleben B, Herbach N, Liu S, Zschiedrich S, Lu S, *et al.* Role of mTOR in podocyte function and diabetic nephropathy in humans and mice. J Clin Invest 2011;121:2197-209.
37. Remuzzi G, Perico N, Macia M, Ruggenenti P. The role of renin-angiotensin-aldosterone system in the progression of chronic kidney disease. Kidney Int Suppl 2005;S57-65. doi: 10.1111/j.1523-1755.2005.09911.x.
38. Chang HF, Hsiao PJ, Hsu YJ, Lin FH, Lin C, Su W, *et al.* Association between angiotensin II receptor type 1 A1166C polymorphism and chronic kidney disease. Oncotarget 2018;9:14444-55.
39. El-Sayed ESM, Abd El-Raouf OM, Fawzy HM, Manie MF. Comparative study of the possible protective effects of cinnamic acid and cinnamaldehyde on cisplatin-induced nephrotoxicity in rats. J Biochem Mol Toxicol 2013;27:508-14.
40. Ho SC, Chang YH, Chang KS. Structural moieties required for cinnamaldehyde-related compounds to inhibit canonical IL-1β secretion. Molecules 2018;23. doi: 10.3390/molecules23123241.
41. Rapa SF, Di Iorio BR, Campiglia P, Heidland A, Marzocco S. Inflammation and oxidative stress in chronic kidney disease—potential therapeutic role of minerals, vitamins and plant-derived metabolites. Int J Mol Sci 2020;21. doi: 10.3390/ijms21010263.
42. Ungurianu A, Zanfirescu A, Nițulescu G, Margină D. Vitamin e beyond its antioxidant label. Antioxidants 2021;10. doi: 10.3390/antiox10050634.